Int. J. Heat Mass Transfer. Vol. 31, No. 7, pp. 1517–1527, 1988
Printed in Great Britain

0017–9310/88 $3.00 + 0.00

An investigation of transient, two-dimensional coupled heat and moisture flow in the soil surrounding a basement wall

LESTER S. SHEN
Underground Space Center, University of Minnesota, Minneapolis, MN 55455, U.S.A.

and

JAMES W. RAMSEY
Department of Mechanical Engineering, University of Minnesota, Minneapolis, MN 55455, U.S.A.

(*Received* 6 *May* 1987 *and in final form* 6 *January* 1988)

Abstract—A two-dimensional finite difference numerical model has been developed to study coupled soil heat and moisture flow around an earth-sheltered construction. Simulations of a basement wall backfilled with a sand and a clay loam were performed. For the sandy soil, a 9% greater wall heat loss during the winter and an increase of over 40% in summer heat gain were observed when the coupling was modelled. The principle mechanism for the greater heat flow was the energy transported by the moisture flow from the ground surface. For the clayey soil, there was no difference between the coupled and uncoupled results.

INTRODUCTION

THE STUDY of earth-sheltered construction has shown that significant energy savings can be achieved by taking advantage of the thermal properties of the surrounding soil. The soil not only acts as a moderator of the cold air temperatures of the winter, but can also provide passive cooling during the summer months. As a result, an opportunity exists for reductions in energy use in both the winter and summer through effective use of the soil. In order to fully realize the total benefits that can be obtained, an understanding of the heat transfer mechanisms through the soil is required.

The study of earth-sheltered construction has primarily focused on heat loss studies through building foundations. In examining insulation strategies of foundation walls and floors, modelers have strictly concerned themselves with heat conduction through the soil, disregarding any moisture flow effects. In these analyses, either a constant value of thermal conductivity is assumed [1, 2] or, in a limited number of cases, some spatial or seasonal variation of the conductivity has been considered [3, 4]. It has been observed, however, that such factors as the soil water thermal conductivity, convection of the soil moisture, and vapor diffusion within the soil pore can result in the soil thermal conductivity varying by more than a factor of eight between dry conditions and 50% saturation [5]. Subsequently, the soil moisture content has a strong influence on the temperature distribution in the soil and, hence, the building heat loss.

Incorporating the influence of soil moisture can greatly complicate the analysis. One of the major factors that influence the moisture distribution in the soil is the temperature field. In general, if a temperature gradient occurs, a moisture gradient will also be evident. The soil moisture content will be lower in the higher temperature region and higher in the lower temperature region. Furthermore, drainage and infiltration also affect soil temperatures. Thus, since the temperature distribution depends on the soil moisture flow and the thermal conductivity, which is also a function of the thermally-driven moisture distribution, the entire problem is one of coupled heat and mass transfer.

The study of coupled heat and moisture transport in soils has been of interest to researchers studying underground power cables, heat storage, nuclear waste disposal, remote sensing, and geotechnical problems [6–13]. While various models have been developed to address these issues, the analysis of earth-contact building surfaces necessitates a certain set of model specifications. This problem requires a two-dimensional numerical code that is capable of handling transient conditions for both saturated and unsaturated moisture flow and heterogeneous soil conditions. This paper will describe the model that was developed and the results that were obtained when the model was used to study the heat flow from a basement wall.

DISCUSSION OF THE NUMERICAL MODEL

The two classical theories that have been used to describe coupled heat and moisture movement in soils were developed by Cary and Taylor [14, 15] and Philip and deVries [16]. The method of Cary and Taylor is a phenomenological model based on irreversible thermodynamics while the Philip and deVries model takes a mechanistic approach. Based on Onsager's relations from irreversible thermodynamics, Cary and

NOMENCLATURE

A	amplitude of the sinusoidal air temperature relation [°C]
B	period of the sinusoidal air temperature relation [rad d^{-1}]
c_l	specific heat of liquid water [J kg^{-1} K^{-1}]
C	volumetric heat capacity of the soil [J m^{-3} K^{-1}]
D_{Ta}	transport coefficient for absorbed liquid flow due to thermal gradients [m^2 s^{-1} K^{-1}]
$D_{T,v}$	thermal diffusivity of vapor [m^2 s^{-1} K^{-1}]
$D_{\psi,v}$	matric head diffusivity of vapor [m s^{-1}]
g	gravitational acceleration [m^2 s^{-1}]
h_{air}	heat transfer coefficient at the earth's surface [W m^{-2} K^{-1}]
K	hydraulic conductivity [m s^{-1}]
L	latent heat of vaporization [J kg^{-1}]
n	day of the year for the sinusoidal air temperature relation [d]
P	phase angle of the sinusoidal air temperature relation [rad]
q_m	moisture flux [kg m^{-2} s^{-1}]
T	temperature [°C]
T_{air}	ambient air temperature [°C]
T_{grd}	deep ground temperature [°C]
t	time [s]
U	U-value of building wall [W m^{-2} K^{-1}]
W	heat of wetting [J kg^{-1}].

Greek symbols

θ	volumetric moisture content [m^3/m^3]
θ_a	volumetric air content [m^3/m^3]
λ	soil thermal conductivity [W m^{-1} K^{-1}]
ρ_l	density of liquid water [kg m^{-3}]
ρ_v	density of water vapor [kg m^{-3}]
ψ	matric potential [m]
ψ_{grd}	matric potential of the deep ground boundary [m].

Subscripts and superscripts

a	air
air	ambient air
grd	ground
l	liquid
m	moisture
T	thermal
v	water vapor
ψ	matric potential.

Taylor developed linear flow equations for describing the soil heat and moisture transport. The advantage of the Cary and Taylor model is that the phenomenological coefficients are experimentally measured and, hence, the exact physical transfer mechanisms need not be explicitly modelled. However, whether these flow equations can be integrated to macroscopic continuum equations requires further proof [16] and limits the approach's usefulness in a transient numerical model.

The method employed by Philip and deVries describes the coupled heat and moisture flow by modelling the physical processes which occur in the soil. While this approach is more suitable for the purposes of this study, the model suffers from an important limitation. Because the moisture flow equation is based on the volumetric moisture content, the model cannot be applied to heterogeneous soils or saturated flow conditions. Milly [17] has developed a model based on the mechanistic approach to cope with these limitations. By rederiving the governing equations using the soil water matric potential as the dependent variable, the study of both heterogeneous domains and saturated/unsaturated flow conditions can be performed. The Milly model also improves upon the Philip and deVries method since it is now capable of handling the exothermic process of wetting, and more properly models the vapor flow within the soil. This is the model that has been adopted for use in this study.

A complete description of the derivation of the coupled governing equations is provided by Milly [18]. The governing equation for soil moisture flow is given by

$$\left[\left(1-\frac{\rho_v}{\rho_l}\right)\left.\frac{\partial\theta}{\partial\psi}\right|_T+\frac{\theta_a}{\rho_l}\left.\frac{\partial\rho_v}{\partial\psi}\right|_T\right]\frac{\partial\psi}{\partial t}+\left[\left(1-\frac{\rho_v}{\rho_l}\right)\left.\frac{\partial\theta}{\partial T}\right|_\psi+\frac{\theta_a}{\rho_l}\left.\frac{\partial\rho_v}{\partial T}\right|_\psi\right]\frac{\partial T}{\partial t}=\nabla\cdot[(K+D_{\psi,v})\nabla\psi+(D_{T,v}+D_{Ta})\nabla T]+\frac{\partial K}{\partial z}. \quad (1)$$

The left-hand side of the equation represents the total water storage (both liquid and vapor) per unit volume of the porous medium. The three terms on the right-hand side describe moisture flow due to water matric potential gradients, thermal gradients, and gravity, respectively.

The soil heat flow is expressed by

$$\left[C+L\theta_a\left.\frac{\partial\rho_v}{\partial T}\right|_\psi-(\rho_l W+\rho_v L)\left.\frac{\partial\theta}{\partial T}\right|_\psi\right]\frac{\partial T}{\partial t}+\left[L\theta_a\left.\frac{\partial\rho_v}{\partial\psi}\right|_T-(\rho_l W+\rho_v L)\left.\frac{\partial\theta}{\partial\psi}\right|_T\right]\frac{\partial\psi}{\partial t}=\nabla\cdot[\lambda\nabla T+\rho_l(LD_{\psi,v}+gTD_{Ta})\nabla\psi]-c_l q_m\cdot\nabla T. \quad (2)$$

The total heat content per unit volume of the soil is given by the left-hand side of equation (2). The heat flow through the soil is governed by conduction (the

first term on the right-hand side of the equation), latent heat transport in the vapor phase and the heat of wetting (the second and third terms in the brackets) and the sensible heat convected by soil moisture flow (the final term).

Although many of the parameters of the coupled heat and moisture equations can be obtained from physical theories and thermodynamic relationships, soil properties such as the soil volumetric heat capacity, C, the thermal conductivity, λ, the permeability or hydraulic conductivity, K, and the functional relationship between the moisture content, θ, and the matric potential, ψ, must be determined for the particular soil being studied. While the basic soil thermal and moisture properties ideally should be determined experimentally, these methods can be quite time consuming and expensive. In the absence of experimental data, some empirical and theoretical models have been proposed which give reasonable predictions for these soil properties. As a result, many of these models have been used in studying heat and moisture flow in soils. Several numerical, analytical, and experimental procedures have been described in the literature [19].

The governing equations of soil heat and moisture transport, as shown by equations (1) and (2), are complex differential equations which defy analytical solution. Not only are the temperature and moisture equations coupled but they are also nonlinear. As a result, solution of the coupled problem requires the use of numerical methods. The solution technique adopted in this study is based on the Patankar–Spalding finite difference method [20]. It is a fully implicit, integrated finite difference technique which has been used with great success in modelling the coupled, nonlinear equations of convective heat transfer and fluid flow problems. The code was written in the Pascal computer language and run on a PDP-11/60 minicomputer.

In order to ensure the validity of the computer model, numerical results were compared to analytically obtained solutions of a number of one-dimensional test cases. Both the conduction and moisture diffusion components of the program were tested. The heat conduction portion was validated against both steady state and transient test cases [21]. The modelling of isothermal moisture flow was verified against a quasi-analytical solution [22]. Results for two soil types were reported by Haverkamp *et al.* [23]. The ability of the numerical model to simulate coupled heat and moisture flow was tested against two cases:

(1) advection and heat dispersion under saturated flow conditions [24];

(2) coupled diffusion of heat and vapor in a very dry soil [25].

Agreement between the model and the analytical solutions was excellent, within 2% in most cases.

After successfully modelling these test situations, the numerical code was used to simulate the temperature and moisture fields that were measured in a 1 m high by 38 cm radius cylinder, filled with a dredged Mississippi River sand. A progression of three experiments were performed with the cylinder. The first experiment was a two-dimensional heat conduction experiment using the dry sand. This experiment provided a well-defined initial temperature distribution throughout the column. After steady state temperature conditions were attained, saturated moisture conditions were imposed at the lower boundary of the cylinder. The second experiment, therefore, studied the effect of one-dimensional moisture vertical infiltration on the temperature distribution. For the third experiment, a constant temperature boundary condition was imposed down the center of the column and two-dimensional coupled heat and moisture transport was studied. The boundary conditions of the column were chosen to be similar to those encountered when modelling earth-contact heat flow from a building.

The models used for calculating the soil thermal properties were in very good agreement with measured data and consequently, good agreement was obtained between the numerical results and the measured temperature distributions for the heat conduction run. Both the transient and steady state distributions could be modelled within 10% of the measured temperatures. Difficulties were encountered measuring the soil moisture profiles for the remaining two experiments. While tensiometers were able to measure the saturated and near-saturated regions of the column, the thermocouple psychrometers placed in the column were unable to give a well-defined moisture distribution for the remainder of the column. However, agreement within 10–15% between the experimentally measured temperature profiles and the numerical model was obtained for all the test cases. Figure 1 shows a comparison of the numerical and experimental radial temperature profiles at various depths in the soil column during day 21 of the one-dimensional heat and moisture transport experiment. Comparison of the numerical and experimental results confirmed that a good description of the soil moisture properties was important when using the numerical model. As long as the soil properties are well defined, the numerical model can provide accurate results when used to analyze earth-contact heat transfer.

SIMULATION OF HEAT AND MOISTURE FLOW AROUND A BASEMENT WALL

After the computer program was tested against the analytical and experimental test cases, the model was used to simulate the moisture and temperature fields surrounding a basement wall. The earth-contact heat flow was modelled using a two-dimensional calculation domain. The soil field was represented by a rectangular domain, 6 m wide and 12 m deep. Along one side boundary, the building wall was simulated. The wall was 2 m in height. Figure 2 shows a schematic of the calculation domain with the temperature and

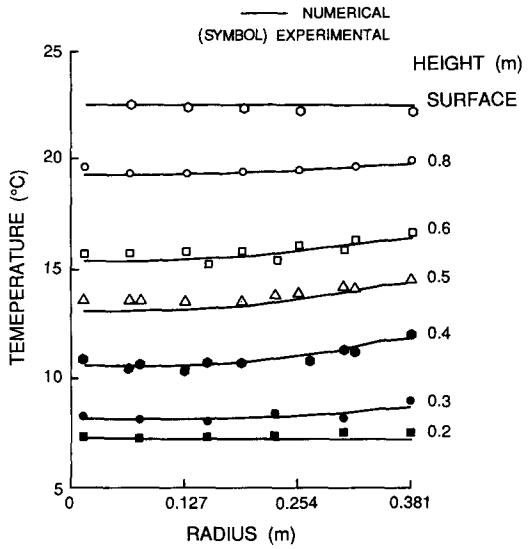

FIG. 1. Radial temperature profiles at various depths in the column for day 21 of the one-dimensional heat and moisture experiment.

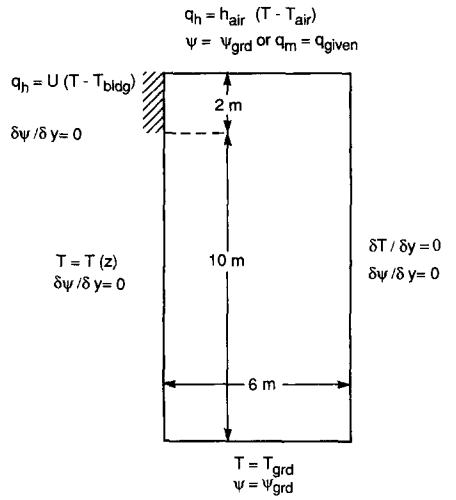

FIG. 2. Boundary conditions for the numerical simulation of the soil surrounding a basement wall.

moisture boundary conditions indicated at each boundary. For the calculation of the temperature field, a constant temperature was imposed at the lower boundary. The temperature was kept at the deep ground temperature, 8.6°C for Minneapolis–St. Paul, Minnesota. This is equivalent to having the water table at a depth of 6 m below the ground surface. At the far side boundary, 12 m from the building, the influence of the building wall can be assumed to be negligible on the soil temperature and an adiabatic boundary condition was imposed. At the upper surface, a convective heat flux boundary condition was used, where the heat flow was governed by the ambient air temperature and the surface heat transfer coefficient. The heat transfer coefficient was obtained from ASHRAE values for an outside surface exposed to a 15 m.p.h. wind [26]. The air temperatures were specified using a regression equation proposed by Kusuda and Achenbach [27]

$$T_{air} = T_{grd} - A\cos(Bn - P) \tag{3}$$

where T_{grd} is the deep ground temperature, A the amplitude of the yearly temperature variation, B the period of the curve, n the day of the year, and P the phase lag. Values of A, B, and P were obtained for Minneapolis–St. Paul from ref. [27]. For the side boundary containing the building wall, the boundary condition at the interface between the soil and the building wall is a heat flux calculated by considering conduction through an uninsulated block wall with natural convection on the inside surface. This expressed as an overall conductance or U-value for the wall multiplied by the temperature difference between the soil/wall interface temperature and the indoor air temperature. The indoor air temperature was held constant at 20°C. Below the wall, a given temperature boundary condition was used. The temperature of the soil was described as a linear function of the depth beneath the building, varying between the building temperature calculated at the base of the wall and the deep ground temperature.

For the moisture portion of the model, the boundary conditions were a constant matric potential at the bottom of the domain and impermeable or zero flux boundaries at the two sides. Initially, the domain was kept at a uniform moisture content. Consequently, the boundary condition at the upper surface was initially maintained at a given matric potential, equal to the deep ground matric potential. At a given time t, the surface boundary condition was changed to a flux boundary condition to simulate infiltration into the soil due to rain. After a short period, the simulated rain was discontinued and the boundary condition was returned to the original constant matric potential condition.

The two-dimensional computer model was used to simulate two types of soils: a sand and a clay loam. The soils that were chosen represent the two extremes of the types of soils normally used as backfill. The soil moisture properties, i.e. the hydraulic conductivity and the moisture characteristic curve, were given as regression equations by Haverkamp *et al.* [23] using a least squares fit on the collected data. The sand was a soil they used for a series of one-dimensional infiltration experiments while the clay loam was the Yolo light clay studied by Philip [22]. For all the simulations, the moisture characteristic curve was considered single valued and hysteresis was ignored.

The initial moisture distribution was a uniform profile with the matric potential set equal to the deep ground value. This was -0.615 m for the sand (or a volumetric moisture content of 0.1 m^3/m^3, 35% of saturation) and -6 m for the Yolo light clay (0.3376 m^3/m^3, 48% of saturation). These were the same initial conditions of Haverkamp *et al.*'s one-dimensional infiltration studies and allowed an intermediate

check with published infiltration results. Furthermore, the comparison with the published one-dimensional infiltration results helped to determine the time step that was needed to perform the simulations. Depending on the rate of infiltration and moisture flow, a maximum time step was determined, above which numerical inaccuracies and instabilities resulted. Since the largest moisture and thermal gradients occurred at the ground surface and near the building, a finer grid spacing was specified in these regions. The grid spacings were determined from the comparison with the infiltration studies and from experience with modelling earth-coupled heat transfer [28].

Since the thermal properties of the two soil types were not given, the thermal conductivity and heat capacity relations were determined by the methods of deVries [29, 30]. The values obtained from the dredged Mississippi River sand were used in defining these properties and the thermal properties were fitted to the moisture content ranges of the two soil types. The remaining soil properties were obtained from the appropriate thermodynamic relationships.

For each soil, two weather conditions were run: during the winter after the air temperature reached slightly above 0°C and during the warmest days of the summer. For Minneapolis–St. Paul, this was around day 92 and day 220 of the year, respectively. Two simulations were performed for each time period. For the first run the computer model was used to simulate the effects of fully coupled heat and moisture flow. During the second run the equations were decoupled. The equations were decoupled so that moisture flow was not influenced by temperature gradients and there was no moisture-driven heat flow. However, the soil thermal conductivity was calculated as a function of the soil moisture content. As a result, the soil thermal conductivity was constant throughout the soil domain for the uniform moisture field and varied as moisture infiltrated into the soil during the rain period. Also during the rain period, the decoupled moisture field would correspond to the one-dimensional infiltration results described by Haverkamp *et al.* The second run provided a gauge of the effect of the coupled heat and moisture flow in the two soils.

In performing the coupled heat and moisture flow simulations, the initial thermal boundary conditions were used to calculate a steady state temperature field. This was used as the initial temperature field. The temperature and moisture fields were then simulated for 7 d to allow for the redistribution of the initial uniform soil moisture profile due to the coupled effects. On day 7, the upper surface moisture boundary condition was altered to simulate rain. The infiltration rate at the surface was held at 2.54 cm h^{-1} for 0.5 h. After that time, the boundary condition was again held at a constant matric potential. The simulation was continued for another 7 d to follow the moisture redistribution and changes in heat flow. For the first 7 d, an hourly time step was used, whereas during the period of infiltration the time step was 30 s. At the end of the rain, the time step was increased progressively until by the end of the day, an hourly time step was again employed. This was maintained for the remainder of the simulation. These runs were performed in this manner for both the sand and the clay during winter and summer weather conditions.

Figures 3(a)–(d) show the results for the winter run using the sandy soil. One-dimensional profiles are shown for the soil temperature, volumetric moisture content, and the wall heat flux. The values for the soil temperature and volumetric moisture content represent the values calculated at the column of grid points in the soil neighboring the domain boundary containing the basement wall. This is 1.0 cm from the wall. Since the effect of coupled heat and moisture flow on the wall heat flux is the focus of this work, the soil temperature and moisture profiles nearest the wall are of prime interest and the use of the one-dimensional profiles permit direct side-by-side comparison to evaluate the coupled effects on the soil temperature, moisture content, and wall heat flux. A two-dimensional soil domain, however, is modelled throughout the simulations. The figures show the profiles at four different times: just before the rain begins, at the time that the rain ends, 18 min after the rain ends, and 5.5 h after the rain has ended. The y-axis of the figure shows the depth into the soil domain where zero is at the surface of the ground. The wall extends down to the 2 m depth and values are plotted for an additional 1 m below the building. The results from the coupled model are shown by a solid line whereas the dashed lines show the uncoupled results.

Just before the rain begins, the results show that the effect of coupling the moisture flow is a reduction in soil temperatures near the wall by as much as 0.8°C or by about 7% of the soil temperatures observed in the decoupled simulations. Comparing the moisture profiles obtained from the two models, soil temperature gradients have caused the moisture to flow away from the building, causing a slight drying out at the wall for the coupled model. Since the upper surface is maintained at a constant moisture content, the dry out produces a moisture gradient from the surface into the ground. This results in moisture flow from the surface and therefore greater penetration of surface temperature effects into the ground. The cooler soil temperatures near the wall indicate that the coupled effect results in greater heat flow from the wall than when the equations are decoupled. The uncoupled model underpredicts the wall heat loss by about 6%, 69.7 W as opposed to 74.5 W.

As the rain ends, the moisture at the surface is near saturation and the wetting front extends about 0.25 m into the soil. Prior to the rain, the soil temperature and heat loss values were nearly identical at the surface for the coupled and uncoupled models, but with the infiltration of the rain a greater drop in temperature at the surface is seen with the coupled model. The temperature of the rain was assumed to be equal to the ambient air temperature. The heat transfer at the

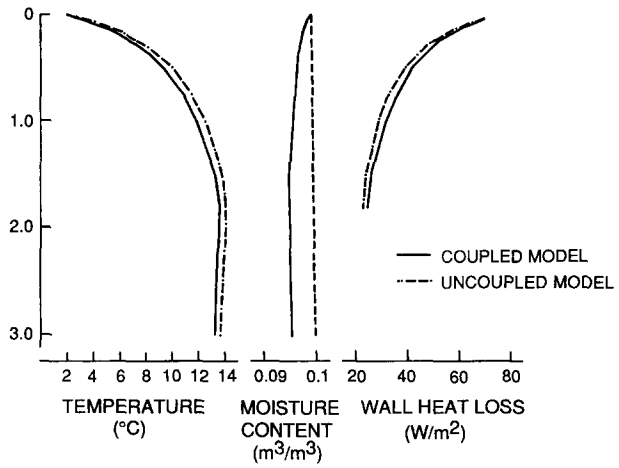

FIG. 3(a). Soil temperature, moisture content, and wall heat loss profiles for a basement surrounded by a sandy soil, day 92.

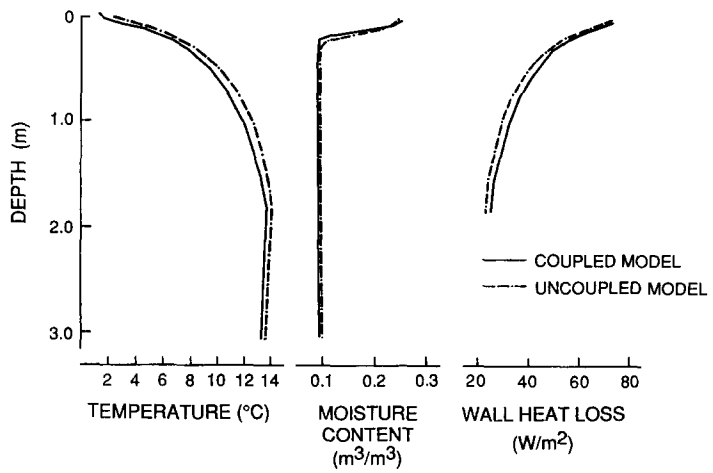

FIG. 3(b). Soil temperature, moisture content, and wall heat loss profiles for a basement surrounded by a sandy soil, day 92 plus 0.5 h (rain at a rate of 2.54 cm h^{-1} occurred for the previous 0.5 h).

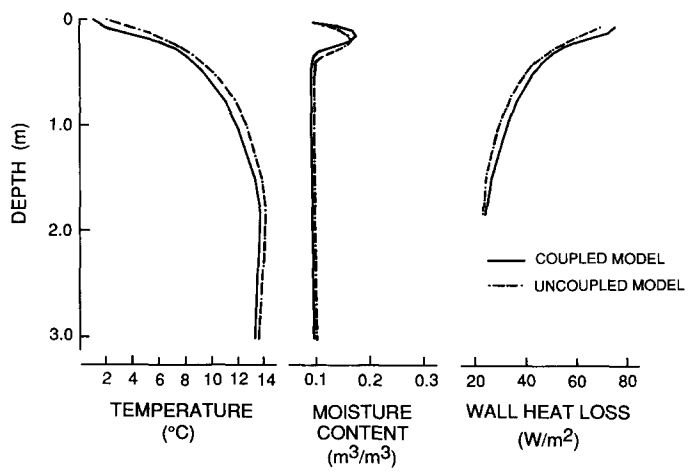

FIG. 3(c). Soil temperature, moisture content, and wall heat loss profiles for a basement surrounded by a sandy soil, day 92 plus 0.8 h (rain ended at 0.5 h).

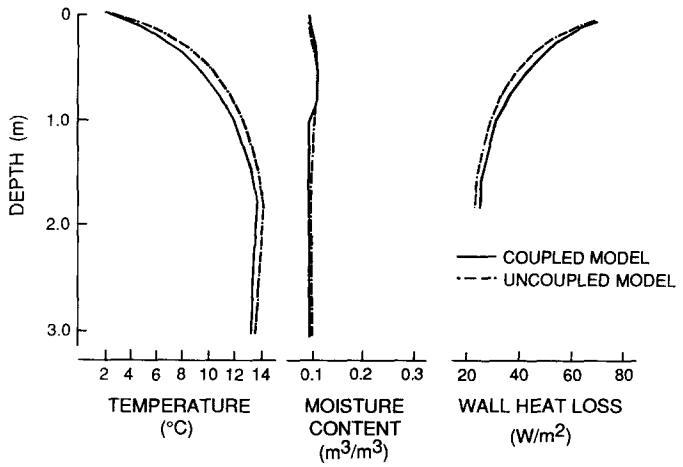

FIG. 3(d). Soil temperature, moisture content, and wall heat loss profiles for a basement surrounded by a sandy soil, day 92 plus 6 h (rain ended at 0.5 h).

surface will increase not only because of high thermal conductivities due to the higher moisture contents but because energy is also transported with the moisture flow. This is not modelled by the uncoupled simulation. An interesting phenomenon is also evident in comparing the moisture profiles of the two models. The moisture profile for the coupled model shows that the temperature gradients near the building oppose the gravitational effects on the moisture to slow the wetting front as it moves into the soil. The wetting front has progressed further into the soil for the uncoupled model. This also causes higher moisture contents at the surface for the coupled model.

Figure 3(c) shows the results after the rain has discontinued for 18 min and the surface moisture boundary condition is again set at a constant matric potential. This was done to approximate the drying that would occur at the surface due to such effects as evaporation and transpiration. The moisture that infiltrated into the soil during the rain now flows in two directions: deeper into the soil due to gravity and away from the building and toward the surface due to temperature gradients and the moisture gradient created by the surface boundary condition. The temperature and heat flux values of the coupled model show a large influence of the infiltration about 10 cm beneath the surface. Again, the temperature gradients at the wall tend to slow the advance of the wetting front. After 5.5 h the wetting front has extended nearly 1 m into the soil (Fig. 3(d)). The surface temperatures and heat fluxes of the two models again are nearly identical and the shapes of the profiles resemble the pre-rainfall profiles. By the end of the day, the rain water near the wall has completely redistributed and the temperature, moisture, and wall heat flux profiles have returned to their pre-rainfall shapes.

Figure 4 shows the time variation of the foundation wall heat loss rate calculated from the two models. The two-dimensional model simulates a 1 m wide section of a wall that is 2 m in height. The results of the coupled model are shown by a solid line and the uncoupled results are given by the dashed line. The results at time zero are the total wall heat losses calculated using the initial steady state temperature field calculated for day 85. During the next 7 d, the wall heat flow is governed by the changing soil temperatures as the surface air temperature increases and, in the case of the coupled model, redistribution of soil moisture. By day 92 the redistribution of the moisture field is near equilibrium for the coupled simulation and, as seen from the results, just prior to the rain the coupled model predicts a 6–7% greater heat loss through the wall.

As the rain begins, the wall heat loss calculated from the coupled model jumps by 1.7 W while the uncoupled results show only a 0.2 W increase. This 0.2 W increase is due entirely to the increase in thermal conductivity. Thus, the energy transported by the infiltrating rain results in a 8.5 times greater increase in wall heat loss than solely the increase in thermal conductivity produced by the rain. The jump in the wall heat loss decreases quickly as the rain distributes and the wetting front becomes less distinct. By the end of the day, the infiltration has almost completely redistributed throughout the domain. The effect of the rain has caused the wall heat loss values to become 9% greater for the coupled model.

The simulation procedure was then performed for the warmest days of the summer. As with the winter runs, rain was simulated for 0.5 h after day 7 of the simulation. The air temperature on day 7 was about 22.5°C. During this summer period, heat flowed into the building since, for most of the 2 m depth, the soil temperatures were greater than the basement air temperature of 20°C. Figures 5(a) and (b) show the soil profiles just before the rain and 18 min after the rain has ended, respectively. Figure 5(a) shows that the high ground surface temperature and the effect of gravity result in slightly higher moisture contents with increasing depth for the coupled model. The influence

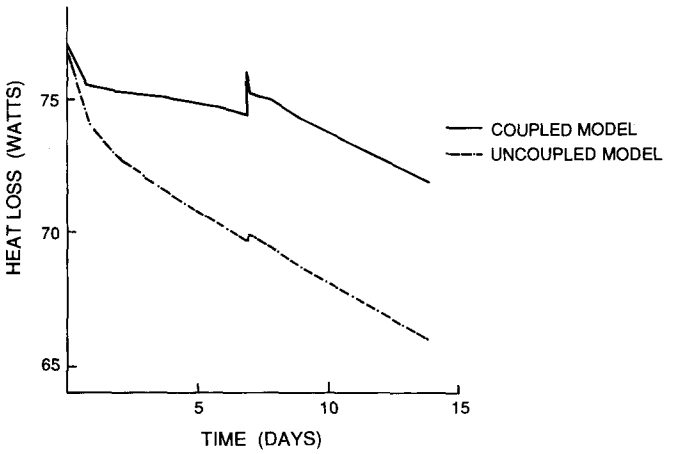

FIG. 4. Total wall heat loss values from day 85 to day 99 for a basement surrounded by a sandy soil.

of the moisture field produces slightly warmer temperatures near the building, causing greater heat gain into the building. For the coupled model, the figure shows heat gain into the building over the entire height of the wall while for the uncoupled model, the base of the wall shows some heat loss. The total wall heat gain for day 220 was 7.5 W for the coupled model and 5.3 W for the uncoupled model, a difference of 42%.

As the rain infiltrates into the soil, the influence of the moisture flow of the temperature and heat flow profiles are similar to the results for the winter. The infiltration of rain produces slightly greater temperatures and heat gain than the uncoupled model. However, during the summer months, the temperature difference between the building and ground surface is much smaller and the moisture profiles are nearly identical for the two models. During the summer temperature gradients act to promote the movement of the wetting front rather than impede it.

Figure 6 shows the full wall heat gain rate through the 1 m wide wall section for the time period of day 213 to day 227 for the two simulations. The infiltration of the rain has a very small effect on the wall heat gain according to the uncoupled results. For the coupled model, the rain causes an increase of about 5% in the heat gain. The summer results show a much more gradual increase in heat flow than was seen during the winter. This is related to the smaller temperature difference between the ground surface and the building. By day 227, the coupled model predicts a heat gain of 8.4 W as opposed to a heat gain of 5.5 W for the uncoupled run.

Simulations were also performed using the moisture properties of the Yolo light clay. The clay has a much lower saturated hydraulic conductivity than the sand (1.23×10^{-7} m s^{-1} as opposed to 9.44×10^{-5} m s^{-1} for the sand) and the moisture characteristic curve will not show as large a decrease in moisture content with increasing matric potential. Thus, moisture would be expected to flow through the soil at a much slower rate than in the sand. For both the winter and summer simulations, the coupled and uncoupled results are essentially identical for the light clay. Only during the winter period do the moisture profiles show a slight difference in value. The rain moves very slowly into the clay. The infiltration of the rain progressed

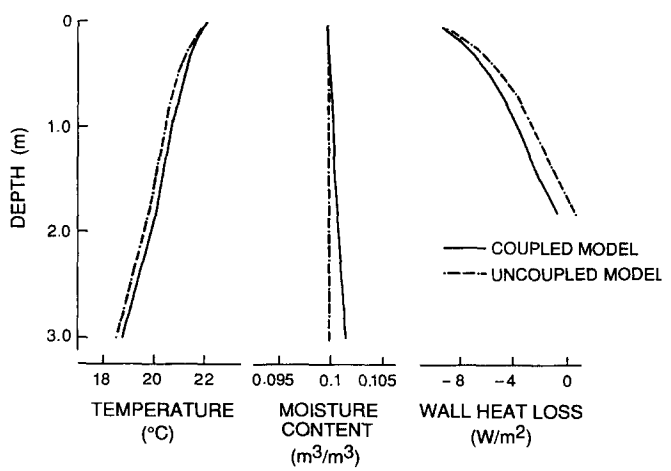

FIG. 5(a). Soil temperature, moisture content, and wall heat loss profiles for a basement surrounded by a sandy soil, day 220.

is ignored. The influence of moisture gradients on building heat flow was found, however, to be dependent on the soil type. For the sand which was a coarse-grained soil, the coupled simulations showed a 9% greater heat flow from the wall during the winter and over a 40% increase in the summer heat gain than for the case when the equations were decoupled. The principal mechanism for the increase in heat flow was the energy transported by the flow of moisture from the ground surface. This moisture flow was due primarily to temperature and gravity effects. For the clayey soil which was a fine-grained soil and, therefore, had a much lower hydraulic conductivity, there was no difference in heat flow values between the coupled and uncoupled results.

Acknowledgements—The authors would like to express their thanks to Professor E. R. G. Eckert and Dr George D. Meixel, Jr. for their valued advice and discussions. This work was supported in part by the Department of Energy under Grant No. DE-AC03-80SF11508 and the National Science Foundation under Grant No. NSF/MEA-8209710.

REFERENCES

1. R. F. Szydlowski and T. H. Kuehn, Analysis of transient heat loss in earth-sheltered structures, *Proceedings of Earth Sheltered Building Design Innovations*, Oklahoma City, Oklahoma (1980).
2. F. S. Wang, Mathematical modeling and computer simulation of insulation systems in below grade applications, *Proceedings of the ASHRAE–DOE Conference on Thermal Performance of the Exterior Envelopes of Buildings*, Orlando, Florida (1979).
3. P. H. Shipp, Thermal characteristics of earth-sheltered structures, Ph.D. Thesis, University of Minnesota, Minneapolis, Minnesota (1979).
4. G. P. Mitalas, Basement heat loss studies at DBR/NRC, National Research Council of Canada, Division of Building Research, Report No. NRCC20416, Ottawa, Canada (1982).
5. J. Mostaghimi and E. Pfender, Measurement of thermal conductivities of soils, *Wärme- und Stoffübertr.* **13,** 3–9 (1982).
6. J. Y. Baladi, D. L. Ayers and R. J. Schoenhals, Transient heat and mass transfer in soils, *Int. J. Heat Mass Transfer* **24,** 449–458 (1981).
7. P. J. Camillo, R. J. Gurney and T. J. Schmugge, A soil and atmospheric boundary layer model for evapotranspiration and soil moisture studies, *Water Resour. Res.* **19,** 371–380 (1983).
8. V. Dakshanamurthy and D. G. Fredlund, A mathematical model for predicting moisture flow in an unsaturated soil under hydraulic and temperature gradients, *Water Resour. Res.* **17,** 714–722 (1981).
9. B. J. Dempsey, A mathematical model for predicting coupled heat and water movement in unsaturated soil, *Int. J. Numer. Analysis Meth. Geomech.* **2,** 19–36 (1978).
10. J. G. Hartley and W. Z. Black, Transient simultaneous heat and mass transfer in moist, unsaturated soils, ASME Paper 81-HT-50, Milwaukee, Wisconsin (1981).
11. P. C. D. Milly, A simulation analysis of thermal effects on evaporation from soil, *Water Resour. Res.* **20,** 1087–1098 (1984).
12. H. S. Radhakrishna, K. C. Lau and A. M. Crawford, Coupled heat and moisture flow through soils, *J. Geotech. Engng* **110,** 1766–1784 (1984).
13. J. P. Schledge, A. B. Kahle and R. E. Alley, A numerical simulation of soil temperature and moisture variations for a bare field, *Soil Sci.* **133,** 197–207 (1982).
14. J. W. Cary and S. A. Taylor, The interaction of the simultaneous diffusion of heat and water vapor, *Soil Sci. Soc. Am. Proc.* **26,** 413–416 (1962).
15. J. W. Cary and S. A. Taylor, Thermally driven liquid and vapor phase transfer of water and energy in soil, *Soil Sci. Soc. Am. Proc.* **26,** 417–420 (1962).
16. J. R. Philip and D. A. deVries, Moisture movement in porous materials under temperature gradients, *Trans. Am. Geophys. Un.* **38,** 222–232 (1957).
17. P. C. D. Milly, Moisture and heat transport in hysteretic, inhomogeneous porous media : a matric head-based formulation and a numerical model, *Water Resour. Res.* **18,** 489–498 (1982).
18. P. C. D. Milly, The coupled transport of water and heat in a vertical soil column under atmospheric excitation, Ph.D. Thesis, M.I.T., Cambridge, Massachusetts (1980).
19. L. S. Shen, An investigation of transient, two-dimensional coupled heat and moisture flow in soils, Ph.D. Thesis, University of Minnesota, Minneapolis, Minnesota (1986).
20. S. V. Patankar, *Numerical Heat Transfer and Fluid Flow*. Hemisphere, New York (1980).
21. H. S. Carslaw and J. C. Jaeger, *Conduction of Heat in Solids*, 2nd Edn, Chap. 5. Clarendon Press, Oxford (1959).
22. J. R. Philip, The theory of infiltration : 1. The infiltration equation and its solution, *Soil Sci.* **83,** 345–357 (1957).
23. R. Haverkamp, M. Vauclin, J. Touma, P. J. Wierenga and G. Vachaud, A comparison of numerical simulation models for one-dimensional infiltration, *Soil Sci. Soc. Am. J.* **41,** 285–294 (1977).
24. F. T. Lindstrom, R. Hague, V. H. Freed and L. Boersma, Theory on the movement of some herbicides in soils; linear diffusion and convection of chemicals in soils, *Env. Sci. Technol.* **1,** 561–565 (1967).
25. J. Crank, *The Mathematics of Diffusion*, p. 306. Clarendon Press, Oxford (1956).
26. *ASHRAE Handbook of Fundamentals*, p. 22.11. ASHRAE, New York (1977).
27. T. Kusuda and P. R. Achenbach, Earth temperatures and thermal diffusivity at selected stations in the United States, *ASHRAE Trans.* **71,** 61–74 (1965).
28. J. W. MacArthur, G. D. Meixel, Jr. and L. S. Shen, Application of numerical methods for predicting energy transport in earth contact systems, *Appl. Energy* **13,** 121–156 (1986).
29. D. A. deVries, Simultaneous transfer of heat and moisture in porous media, *Trans. Am. Geophys. Un.* **29,** 909–916 (1958).
30. D. A. deVries, *Thermal Properties of Soils, Physics of Plant Environment* (Edited by W. R. Van Wijk). Wiley, New York (1963).

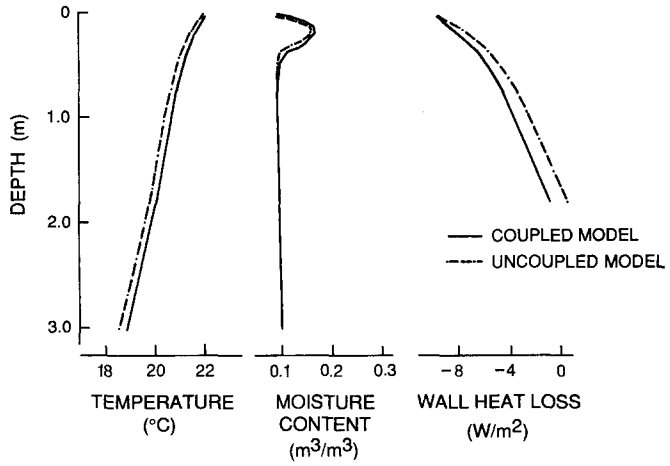

FIG. 5(b). Soil temperature, moisture content, and wall heat loss profiles for a basement surrounded by a sandy soil, day 220 plus 0.8 h (rain at a rate of 2.54 cm h^{-1} occurred for 0.5 h, ending at 0.5 h).

less than 0.25 m into the soil by the end of the day during both the winter and the summer. In contrast, for the sand, the wetting front had flowed nearly past the entire length of the wall and almost completely redistributed by the end of the day. Thus, the effect of coupled heat and moisture flow is very small for the clay.

Figure 7 shows the change in total wall heat loss rate during the winter period for the clay as compared to the results of the coupled model for the sand. The effect of the rain is very small on the heat loss into the clay soil. The large difference between the two soils is a result of the differences in the thermal conductivities and the larger influence of coupling with the sand. At corresponding moisture contents, a clay will exhibit lower thermal conductivities than a sand. Thus, even though the clay is at about 50% saturation and the sand is at 35% saturation, the clay has a lower thermal conductivity and lower heat losses are seen.

From the results observed, neglecting the effect of coupled heat and moisture flow resulted in underestimation of heat loss by 9% in the winter and over 40% in the summer for the sandy soil. The energy transported by the flow of moisture from the surface is the principal reason for this discrepancy. The effect is much more pronounced with coarse grained soils where the moisture can flow through rapidly. With fine grained soils as a clay loam, the low hydraulic conductivity will result in a negligible effect resulting from the coupled phenomena.

The results of these initial studies show that for certain soil types the effect of moisture flow on foundation heat loss can be appreciable, particularly during the summer months. Consequently, an opportunity for energy savings may be possible depending on the choice of the backfill soil. With the ability to model non-homogeneous soil domains, examination of different backfill and drainage strategies may reveal new energy saving possibilities.

CONCLUDING REMARKS

The results of this study show that the heat flow from an earth-sheltered construction can be underpredicted if the coupled effect due to moisture flow

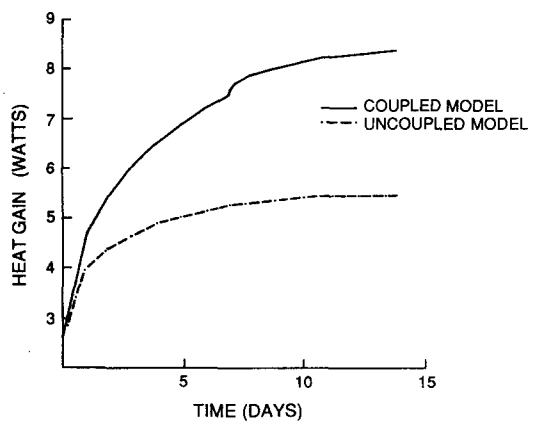

FIG. 6. Total wall heat gain values for day 213 to day 227 for a basement surrounded by a sandy soil.

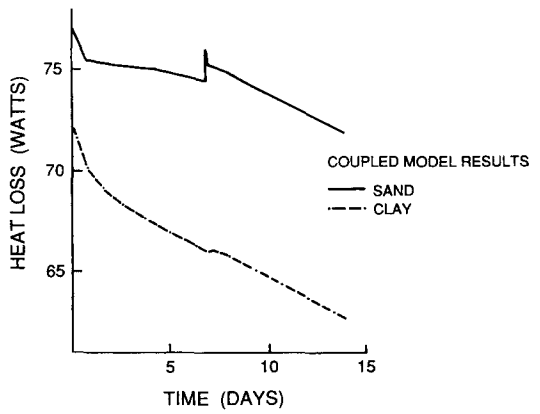

FIG. 7. Comparison of total wall heat loss values from day 85 to day 99 of a basement wall surrounded by a sandy soil and Yolo light clay.

ETUDE DU TRANSFERT BIDIMENSIONNEL COUPLE DE CHALEUR ET D'HUMIDITE DANS LE SOL ENTOURANT UN MUR DE FONDATION

Résumé—On développe un modèle numérique bidimensionnel aux différences finies pour étudier le transfert couplé de chaleur et d'humidité dans le sol autour d'une construction. On réalise des simulations d'un mur de fondation rempli avec du sable ou de l'argile. On observe pour le sable une perte de chaleur accrue de 9% pendant l'hiver et un gain de chaleur augmenté de 40% pendant l'été. Le mécanisme principal pour ce plus grand transfert de chaleur est le transfert d'énergie par le transfert d'humidité à partir de la surface. Pour le sol d'argile, il n'y a pas de différence entre les résultats avec couplage ou sans couplage.

UNTERSUCHUNG DES INSTATIONÄREN ZWEIDIMENSIONALEN GEKOPPELTEN WÄRME- UND FEUCHTETRANSPORTS IM ERDREICH AN EINER KELLERWAND

Zusammenfassung—Es wurde ein zweidimensionales numerisches Finite-Differenzen-Modell zur Untersuchung des gekoppelten Wärme- und Feuchtetransports in der Umgebung einer ins Erdreich eingelassenen Konstruktion entwickelt. Es wurden Simulationsrechnungen für eine mit Sand und tonigem Lehm hinterfüllten Wand durchgeführt. Für die mit Sand hinterfüllte Wand wurde ein um 9% größerer Wärmeverlust im Winter und ein Anstieg des Wärmerückgewinns von über 40% im Sommer beobachtet. Bei größeren Wärmeströmen dominierte der Energietransport durch Feuchtewanderung von der Erdoberfläche. Für lehmige Erde konnte kein Unterschied zwischen den Ergebnissen nach der gekoppelten und ungekoppelten Lösung beobachtet werden.

ИССЛЕДОВАНИЕ НЕСТАЦИОНАРНЫХ ДВУМЕРНЫХ ВЗАИМОСВЯЗАННЫХ ПОТОКОВ ТЕПЛА И ВЛАГИ В ПОЧВЕ, ОКРУЖАЮЩЕЙ ФУНДАМЕНТ

Аннотация—Разработана двумерная конечно-разностная модель для изучения связанных потоков тепла и влаги вокруг конструкций, встроенных в землю. Проведено численное моделирование стены фундамента, засыпанной песком и суглинком. Для песчаной почвы учет взаимосвязанности потоков тепла и влаги приводил к 9% потере тепла в зимний период и 40% возрастанию теплового потока летом. В случае суглинистой почвы различий между результатами для связанных и несвязанных потоков не наблюдалось.